Enzyme and Microbial Technology 123 (2019) 30–38

Contents lists available at ScienceDirect

Enzyme and Microbial Technology

journal homepage: www.elsevier.com/locate/enzmictec

An improved enzyme nanoparticles based amperometric pyruvate biosensor for detection of pyruvate in serum

Mansi Malik[a], Reeti Chaudhary[a], Chandra Shekhar Pundir[b,*]

[a] Department of Biotechnology, Deenbandhu Chhotu Ram University of Science and Technology, Murthal, Sonipat, Haryana, India
[b] Department of Biochemistry, M.D. University, Rohtak, Haryana, India

ARTICLE INFO

Keywords:
Pyruvate oxidase nanoparticles
Pyruvate biosensor
Gold electrode
Serum

ABSTRACT

The nanoparticles of commercially available pyruvate oxidase (POx) from *Aerococcus* species were prepared by desolvation method, which were then characterized and covalently immobilized onto gold electrode (AuE) to construct an improved model of amperometric pyruvate biosensor. The POxNPs/Au electrode was analyzed morphologically by scanning electron microscopy (SEM). On the other hand, cyclic voltammetry studies (CV) and electrochemical impedance spectroscopy (EIS) helped in deciphering the electrochemical properties of the electrode at different stages of construction. The biosensor showed optimum response within 7.5 s, at a potential of 0.28 V, pH 5.5 and 35 °C. A linear relationship was observed between biosensor response i.e. current (μA) and pyruvate concentration in the range, 0.01 μM - 5000 μM, with a lower detection limit of 0.67 μM. The analytical recovery of added pyruvate in sera was 99.0% and 99.5% within and between batch coefficient of variation (CV) were 0.045% and 0.040% respectively. The working electrode displayed an excellent correlation coefficient (R^2 = 0.99%) between levels of pyruvate in sera, as detected by the standard spectrophotometric method and the present biosensor. The biosensor was utilized for detection of total pyruvate level in sera of apparently healthy individuals and patients suffering from cardiogenic stress, more specifically cardiac failure. The activity of the biosensor deteriorated by 25%, after its regular use over a period of 240 days, while being stored dry at 4°C.

1. Introduction

Pyruvate ($C_3H_4O_3$) is an alpha- keto organic molecule prominently found in cellular components of every living cell [1]. It is known to be the key molecule involved in various metabolic pathways including glycolysis, which are further involved in biological energy production under aerobic and anaerobic conditions as per the situation encountered by the cell [2]. Normal levels of pyruvate found in the blood lies between 40–120 μM [3]. These levels are known to fluctuate from the normal levels in several diseased conditions [4]. Pyruvate is an intermediary metabolite in carbohydrates, protein as well as fat metabolism and, due to this reason the ability to measure intermediary metabolites in blood is becoming increasingly important [5]. Over the past 20 years, researchers have been trying to find a means to detect pyruvate, which has important applications in clinical, bioprocess, food and diagnosis [6]. The level of pyruvic acid plays an important role in sustaining fuel homeostasis [7]. The higher levels of plasma pyruvate demonstrate the PDHC (pyruvate dehydrogenase complex) deficiency, which thereby results in inadequate removal of pyruvate and generation of lactate leading to insufficient energy production. Thereby, increased levels of pyruvate are known to play a prominent role in autism [8]. Pyruvate is also known to exhibit cardiac muscle inotropic and bariatric activity. The study of biochemical changes in cardiac failure is a fascinating field of study in the hemodynamics. Recent research also depicted that pyruvate plays a major role in cardiovascular diseases and coronary infarction [9]. The levels of pyruvate, along with glucose and L- lactate, in blood are related to diabetes mellitus [3]. In view of these factors, there is an urgent need to develop a simple, sensitive, rapid and reliable method for determination of pyruvate in blood. Various methods are elucidated in the literature for determination of pyruvate such as colorimetric [10], spectrophotometric [11], enzymic- fluorimetric [1,12] and high- performance liquid chromatography (HPLC) [13]. However, these methods are cumbersome involving sluggish and stiff sample pre- treatment steps, exorbitantly priced instrumental set- up along with, skilled persons to operate with large volumes of blood samples [1]. Biosensors offer an enticing alternative to overcome these pitfalls. Biosensors are analytical devices that utilize the sensitivity and specificity of the biological

* Corresponding author.
E-mail address: chandraspundir@gmail.com (C.S. Pundir).

https://doi.org/10.1016/j.enzmictec.2019.01.006
Received 13 November 2018; Received in revised form 24 December 2018; Accepted 8 January 2019
Available online 11 January 2019
0141-0229/

Table 1
A comparison of various analytical parameters of pyruvate biosensors.

S. No.	Type	Composition of electrode	Method of immobilization	Working potential (mV) Ag vs AgCl	Response time (seconds)	Optimum pH	Optimum incubation temperature (^{0}C)	Working range (μM)	LOD (μM)	Sensitivity	Precision (%) or linearity	Storage life (Days)	Samples in which applied	Reference
1.	Amperometric	3-MPA/6-ACA/POx glutaraldehyde modified AuE	Cross linking	70	6	6.0	ND	ND	1.87	ND	0.62	ND	ND	[2]
2.	Amperometric	Methylene green- mediated pyruvate electrode based on POx entrapped in carbon paste	ND	ND	ND	7.0	ND	12000-16000	ND	518	ND	> 60	Human sweat	[3]
3.	Fluorimetric	Microvolume fluorescence capillary	Cross linking	ND	ND	6.0	30	4-120	0.87	ND	2.92	32(50% loss)	human sera	[5]
4.	Amperometric	POx immobilized on meldolas blue electrode	Adsorption	150	ND	5.7	ND	2-12 μM	1-2	ND	ND	ND	Pungency in onions (Allium cepa L.)	[6]
5.	Amperometric (Polarographic)	POx immobilized in gelatin on YSI type dissolved oxygen probe	Cross linking	800	180	7.0	35	ND	ND	ND	0.0025-0.05	ND	ND	[9]
6.	Amperometric	POx immobilized onto Pt disc electrode	Cross linking, adsorption & entrapment	600	ND	6.5	ND	10- 5000	ND	31.06 nA/mM	ND	14 (50% loss)	Biological fluids	[18]
7.	Amperometric	Redox hydrogel	Adsorption	400	ND	6.0	ND	2- 6	30 μM	0.26 nA/mM	ND	ND	Calf serum	[19]
8.	Amperometric	POx electrodeposite-d polytyramine	Covalent attachment to polytytramine	650	ND	7.2	ND	5 μM-5000	50	0.4 μA mM^{-1}	Linearity 0.1-3.0 mM	90 (No loss)	Serum Samples	[20]
9.	Amperometric	POx immobilized in gelatin (pO_2 electrode)	Tanning with glutaraldehyde	ND	ND	7.0	30-35	ND	ND	ND	2.5 at 30^0 & 1.7 at 35^{0}C	ND	Blood and Yoghurt	[21]
10.	Amperometric	POx alongwith polyneutral red redox immobilized onto carbon electrode	Cross linking	250 vs SCE	ND	ND	ND	90-600 μM	34	ND	Linearity 0.6 mM	14 (38% loss)	Onion and garlic	[22]
11.	Amperometric	Redox polymer /oxiodreductasenanocomposite thin films of silicon dioxide/ silicon and flexible mylar substrates on photographical-ly patterned Au microelectrodes	Chemisorption	0-500	20	ND	ND	0-2000	ND	0.133	ND	ND	ND	[23]
12.	Amperometric	POx coimmob-ilized in a series of polymeric dialysis membranes	Physical adsorption	650	ND	ND	ND	ND	ND	6mM (linear response)	ND	5 hrs (25% loss) at 4^0 C	ND	[24]
14.	Amperometric	POx immobilized onto a porous acetyl-cellulose membrane	Adsorption	ND	120	7.0	ND	ND	ND	ND	ND	> 10	NR	[25]
13.	Amperometric	POx containing poly(vinyl alcohol)/ polyion complex- bilayer membrane onto gold disc electrode	Cross linking	150 -300	ND	ND	ND	ND	0.05	ND	ND	7 (50% loss)	NR	[26]
15.	Amperometric	POxNPs/AuE	Covalent immobilization	280	7.5	5.5	35	0.01-5000	0.67	ND	0.99	240	Sera	Present biosensor

Abbreviations: 3-MPA/6-ACA - 3-mercaptopropionic acid/6-aminocaproic; POx- Pyruvate Oxidase.

molecules in cooperation with electrochemical transducer elements to display tedious bio-analytical measurements with ease, simplicity and precise to use formats [14]. From the literature cited till now, the enzyme POx has been immobilized onto several variants of nanomaterial-based electrodes, all of which are summarized in Table 1 consisting 14 references. However, these nanocomposites modified electrodes embrace complex strategies for construction of working electrode. Further, direct immobilization of the native enzyme causes several drawbacks like enzyme denaturation, loss of enzyme stability and activity thereby retarding the performance of the biosensor. In recent years, enzyme nanoparticles (ENPs) are being employed due to their enhanced and exceptional electrical, thermal, mechanical and optical properties. The choice of gold (Au) as an electrode offers several enticing advantages in terms of good conduction of electrons through its surface, easy availability and low background noise. Therefore, the main key feature of this work is the preparation of NPs of pyruvate oxidase (POx), their characterization and direct covalent immobilization of these ENPs onto Au electrode, which has overcome several audacities presented by the direct immobilization of the native enzyme [15]. The present biosensor has also shown improved analytical performance and employed for determination pyruvate in sera of cardiac patients.

2. Materials and methods

2.1. Chemicals and reagents

Pyruvate oxidase (POx) from Aerococcus species (100 U/mg), sodium pyruvate pure ($C_3H_3O_3Na$), alumina silica slurry from SRL Religare, Mumbai; thiamine pyrophosphate (TPP), magnesium chloride ($MgCl_2$) and flavin adenine dinucleotide (FAD) from Sigma- Aldrich (St. Louis, MO, USA), 2.5 cm gold wire (23 carat) of uniform diameter of 2.5 mm, was bought from a local jeweler's shop. All other chemicals were of analytical reagent (AR) grade. Double distilled water (DW) was used throughout the experiment. Sera samples of evidently healthy subjects and persons suffering from cardiogenic stress were procured from Pandit Bhagwat Dayal Sharma Post Graduate Institute of Medical Science Hospital, Rohtak and Holy Heart Hospital, Rohtak and Noble Heart Hospital, Rohtak.

2.2. Equipment used

Potentistat/ Galvanostat (Autolab, AUT83785, Eco Chemie, The Netherlands) with NOVA 1.4 software incorporating a three- electrode system comprising of POxNPs/AuE as working electrode, Ag/ AgCl as a standard and Pt wire as an auxiliary electrode. Transmission electron microscope (TEM) (Jeol, JEM 1011), Scanning electron microscope (SEM) (Zeiss EV040, USA), Fourier transform infrared (FTIR) spectrometer (Bruker, OPUS 6.5 software), UV–vis spectrophotometer (Lab India Analytical, UV 3092), were used. The electrochemical impedance spectra (EIS) was recorded in potentiostat by NOVA 1.4 (FRA) software in 5 mM potassium ferrocyanide/ potassium ferricyanide solution at 0.28 V in a frequency range of 0.01 Hz to 10^4 Hz.

2.3. Assay of pyruvate oxidase

The modified method elucidated by Dagar and Pundir [16], was implemented to assess the activity of POx. The reaction mixture contained 10 µl each of 10 mM TPP, 1 mM $MgCl_2$ and 1 µM FAD accompanied by the addition of 0.1 mM pyruvic acid in 1.5 ml reaction buffer (0.05 M potassium phosphate buffer, pH 7.0) in a test tube. This step was carried out in a dark environment. After pre- incubation at 40 °C for 5 min, the reaction was started by adding 0.1 ml of dissolved POx in reaction buffer, whilst control contained DW in place of POx solution. After incubation at 40 °C for 10 min in dark, 1.0 ml of cold reagent (50 mg of 4- aminophenazone, 100 mg solid phenol and 1.0 mg of horseradish peroxidase dissolved in 100 ml of 0.4 M sodium phosphate buffer, pH 7.0) was added to reaction mixture and kept at room temperature in dark for 30 min to develop pink color. A_{520} was read against control. The color reagent was stored at 4°C, when not in use.

2.4. Fabrication of POxNPs modified gold electrode

2.4.1. Preparation of POx nanoparticles (POxNPs)

POxNPs were prepared by the desolvation method [17]. To 1.0 ml of POx solution (1 mg/ ml) 4.0 ml of absolute ethanol was added drop wise at the rate of 0.1- 0.2 ml/ minute under continuous stirring at a speed of 500 rpm. Thereafter, 1.8 ml of 2.5% glutaraldehyde was added to the above mixture under similar stirring conditions at 4°C for 24 h to enable cross- linking of ENPs. The glutaraldehyde crosslinked POxNPs suspension was centrifuged at 1200 *g* (5000 rpm) for 10 min at 4°C, followed by redispersion of ENPs in 2 ml of 0.1 M sodium phosphate buffer, pH 7.0 and sonication for 5 min. The obtained ENPs were thiol functionalized by adding 0.12 *g* of cysteamine solution under continuous stirring for 5–6 hr. POxNPs were isolated by centrifugation at 1200 *g* for 10 min at 4°C. It was supposed that aldehyde groups of glutraldehyde cross linked ENPs reacted with the alpha $–NH_2$ groups of cysteamine through Schiff base. The functionalized POxNPs were stored at 4°C until use.

2.4.2. Characterization of POxNPs

UV- Vis spectra (200–600 nm) of POxNPs was recorded to confirm the formation of the ENPs. The POxNPs were morphologically characterized by taking their images under a TEM. FTIR spectra (4000- 400 cm^{-1}) of POxNPs was also recorded to confirm the formation of ENPs.

2.4.3. Construction of working electrode (POxNPs/ AuE)

A bare gold electrode (AuE) was cleaned with alumina silica slurry (diameter- 0.05 µM) using a polishing cloth to remove unwanted debris adhering to the surface of the bare AuE. Further, AuE was dipped in a heterogeneous mixture of piranha solution (3:1 = H_2SO_4:HNO_3) and treated thereafter, with alcohol to functionalize with −OH group. Next, the cleaned AuE was placed into POxNPs suspension under mild stirring at 4°C for 24 h. This allowed the immobilization of the cysteamine functionalized POxNPs onto the polycrystalline Au electrode through thiolate/ covalent bond between – SH group of ENPs and and −OH group of Au electrode (Fig.1). The POxNPs/ Au electrode or the working electrode was then washed 4 times with 0.1 M sodium phosphate buffer (pH- 7.0)(SPB) and stored in this buffer, when not in use at 4°C. The morphological pattern of the working electrode was analyzed by SEM whereby, CV and EIS was analyzed to record the electrochemical pattern.

The amperometric pyruvate biosensor undergoes various enzymic and electrochemical reactions (Fig.1):

$$\text{Pyruvate} + O_2 + P_i \rightarrow \text{Acetyl phosphate} + CO_2 + H_2O_2 \text{ (in the presence of POx)}$$

$$H_2O_2 \rightarrow 2H^+ + O_2 + 2\,e^- \text{ (under high voltage)}$$

2.4.4. Construction and testing of amperometric pyruvate biosensor

A schematic representation of fabrication of POxNPs/Au electrode and electrochemical reactions involved in its response measurement is presented in Fig. 1. Wherein, an amperometric pyruvate biosensor was fabricated where POxNPs/ Au electrode acted as a working electrode with Ag/ AgCl as reference electrode and Pt wire as an auxiliary electrode and was connected through potentiostat/ galvanostat. The biosensor was tested electrochemically by studying cyclic voltammetry (CV) in 0.1 M phosphate buffer consisting optimized concentrations of the substrate and co- factors (0.1 ml of 20 mM pyruvate, 10 µl of 10 mM TPP, 10 µl of 1 mM $MgCl_2$ and 10 µl of 1 µM FAD) at a scan rate of 30 mV^{s-1} at an applied potential range of -0.6 to + 0.6 V. The current was recorded in µA at different time intervals with a gap of 2.5 s.

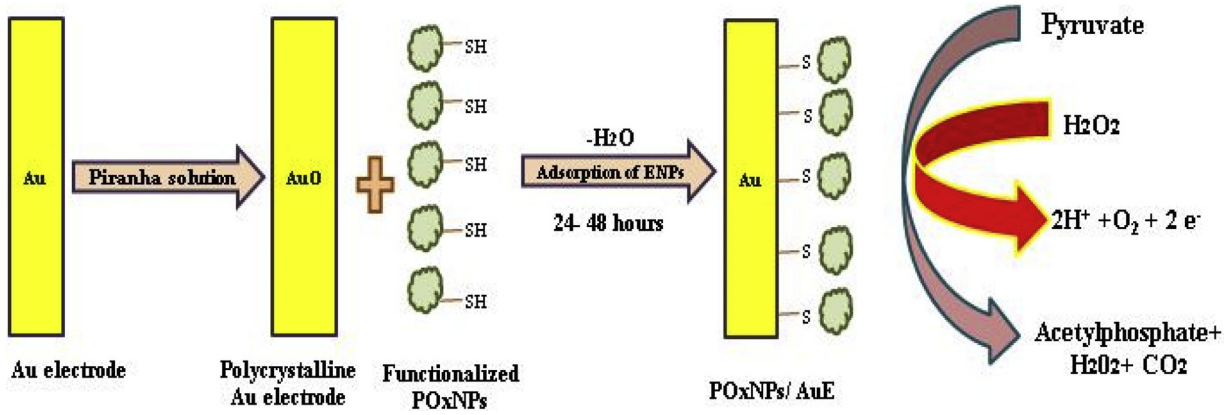

Fig. 1. Schematic representation of electrochemical reactions involved in the construction of POxNPs/AuE (POxNPs- Pyruvate Oxidase Nanoparticles; AuE- Gold electrode).

2.5. Optimization of pyruvate biosensor

For carrying out the optimization studies, several kinetic parameters of the POxNPs modified Au electrode such as optimum pH, temperature, response time and effect of substrate (pyruvate) concentration were analyzed amperometrically. Various buffers within a range of pH 4.0–9.0 were prepared at an interval of 0.5 with a final concentration of 0.1 M. Similarly, incubation temperature (15–50°C) and time (1–10 s) were optimized. The effect of pyruvate concentration on biosensor response was studied by varying the pyruvate concentration in the range of 0.1–5000 μM. The limit of detection (LOD) was calculated by using following the equation:

$$LOD = 3 \times \sigma / \text{slope}$$

where, σ- Standard deviation of response

2.6. Amperometric determination of pyruvate in serum

Blood samples (1 ml each) from apparently healthy adults and patients suffering (males and females separately) from cardiogenic stress between the age group 30–90 years, were collected from local hospitals (PGIMS, Rohtak, Holy Heart, Noble Heart, Rohtak). These collected samples were left for 1 h at RT, and thereafter, centrifuged for 5 min at 5000 rpm, and the resultant supernatant (sera) was collected and stored at 4°C until use. The amount of pyruvate in sera was determined by the present biosensor synonymously as illustrated for the response measurement studies under the optimized working conditions, except that pyruvate was replaced by serum. The concentration of pyruvate was interpolated between pyruvate concentrations and current (μA).

2.7. Evaluation of pyruvate biosensor

The analytical performance of the biosensor was evaluated by analyzing the linearity, limit of detection (LOD), analytical recovery, coefficient of variation (CV) and correlation coefficient (R^2) of biosensor. The effect of several interferants found in the blood such as uric acid, urea, ascorbic acid, glucose was studied at their physiological concentrations.

2.8. Applications of pyruvate biosensor

The samples of blood from apparently healthy individuals and diseased patients were collected in a plastic vial and these were then left to coagulate for 1 h by keeping them undisturbed at RT. These serum samples were then centrifuged for 20 min at 1200 *g* to separate the cellular fractions, and the resultant supernatant was procured. Each serum sample was scrutinized for pyruvate content at a potential of +0.28 V, in 25 ml SPB buffer (pH- 5.5) containing 0.1 ml of serum samples along with the necessary co-factors (10 μl each) and its maximum current was recorded. The amount of pyruvate in sera was calculated from the standard curve between pyruvate concentrations and biosensor response in current as measured by the present biosensor under optimum conditions.

2.9. Reusability of the working electrode

The reusability and storage stability of the biosensor was investigated at an interval of 30 days over a period of 240 days.

3. Results and discussion

3.1. Characterization of POxNPs

3.1.1. Characterization of POxNPs by TEM, UV–vis and FTIR

The size of POxNPs as observed in the images recorded by TEM varied between 7.78 nm–24.80 nm (Fig.2a) and displayed an average size of 15.77 nm, thereby enhancing the surface area of the electrode as compared to that of the native enzyme. UV–vis spectrum of POxNPs unveiled an intense absorbance peak at 280 nm, explaining the presence of amino acids with aromatic rings of native enzyme moieties following their subsequent aggregation into nanoparticles. The aggregation of free/native enzyme molecules into nanoparticles led to increase in absorption at 280 nm. (Fig.2b). The FTIR analysis revealed the spectrum of native POx and POxNPs, whereby the native enzyme showed characteristic peaks at 3330, 2132, 2028, 1636 cm^{-1} (Fig.2c). These high and low transmittance peaks could be attributed to the various functional groups present in the enzyme moiety. The wider band (at 3330 cm^{-1}) points to the existence of amine group in the structure. The analysis of the POxNPs by FTIR spectrum (4000- 400 cm^{-1}) displayed characteristic peaks at 3330, 2132, 2028, 1636 cm^{-1}, which could be assigned to O—H stretching demonstrating the —OH group, and the combined peaks at 2132 cm^{-1} and 2028 cm^{-1} were prominently visible due to stretching vibrations of C═C and C═N groups respectively and peak at 1636 cm^{-1}showed C═O stretching. A major shift in these characteristic peaks is visible in FTIR spectrum of POxNPs, which can be caused due to treatment with ethanol, glutaraldehyde and cysteamine. On comparison with the FTIR spectra of native POx and POxNPs, POxNPs showed an extra sharp peak at 1076 cm^{-1} indicating the addition of $–NH_2$ groups after treatment with cysteamine.

3.1.2. Characterization of working electrode (POxNPs/AuE) by SEM

The SEM images with a stepwise modification of the surface of bare AuE and the working electrode are shown respectively (Fig. 3). The SEM images of the bare AuE revealed a homogenous and even pattern.

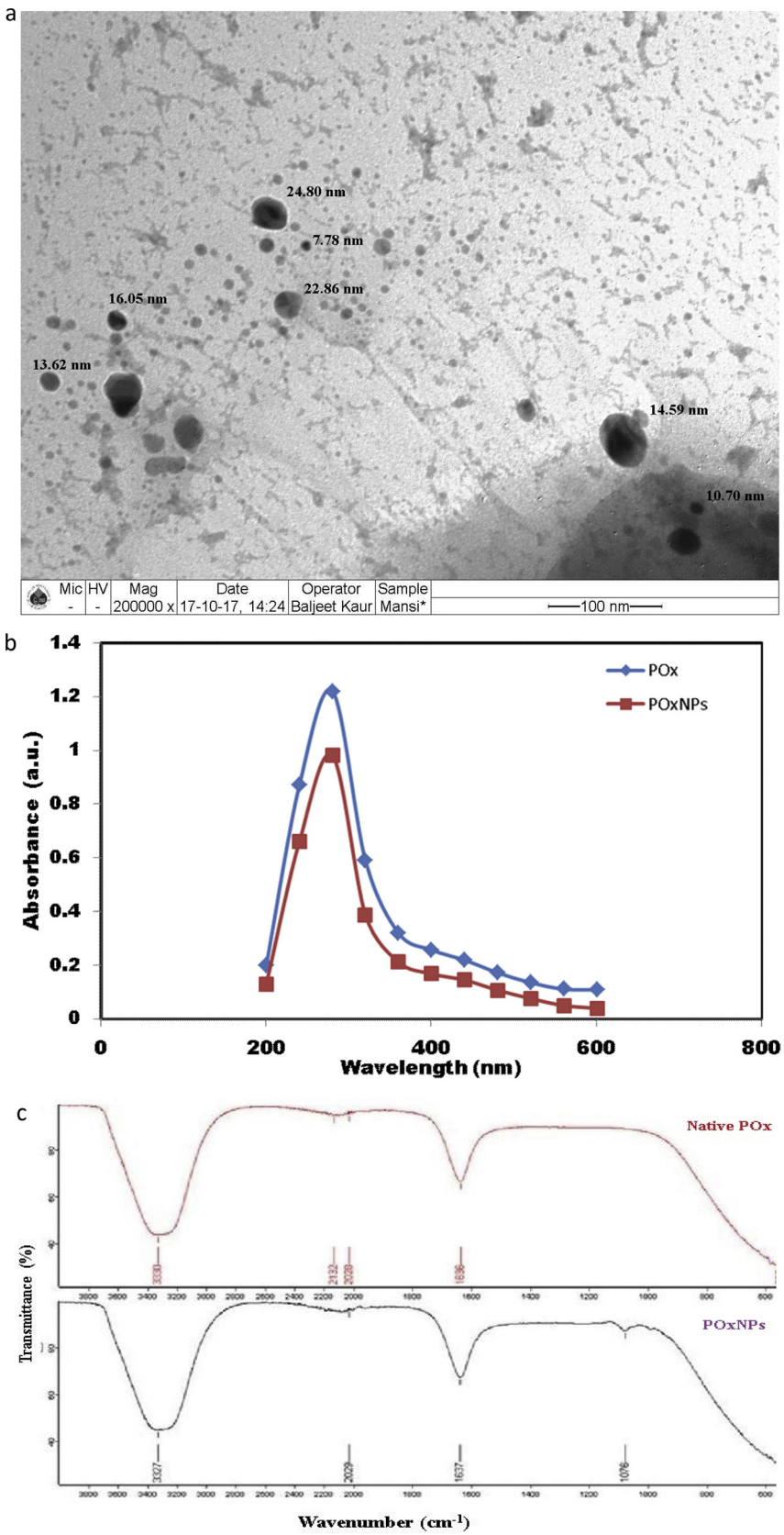

Fig. 2. (a) Transmission electron microscopy (TEM) images of nanoparticles of enzyme Pyruvate Oxidase.(b) UV–vis spectra of POx and POxNPs (POx- Pyruvate oxidase; POxNPs- Pyruvate Oxidase Nanoparticles).(c) FTIR spectra of native enzyme POx and POxNPs.

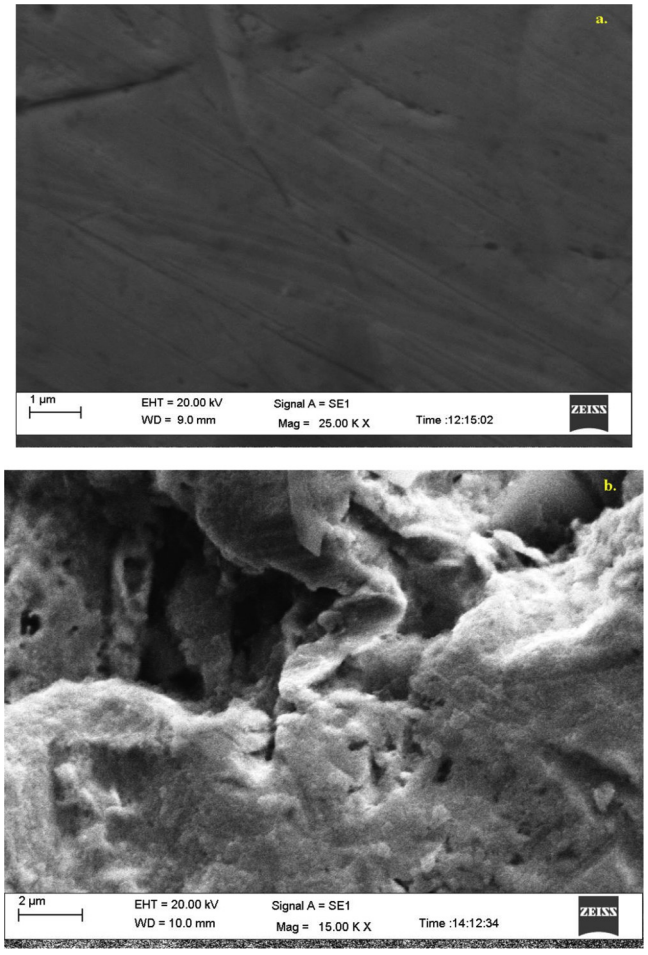

Fig. 3. Scanning electron microscopic images (SEM) images of (a) bare gold electrode (b) POxNPs modified AuE.

Whilst, on the contrary, the working electrode exhibited irregular morphological pattern displaying beaded and globular structures, which were visible due to adsorption of POxNPs onto the Au electrode. The POxNPs/AuE displayed enhanced surface area after adsorption of POxNPs.

3.1.3. Voltammetric response of POxNPs/Au electrode

The amperometric response of bare AuE and the POxNPs/AuE was recorded (Fig. 4a). The bare AuE did not show any prominent oxidation and reduction peak, while, POxNPs/AuE exhibited remarkably visible and clear oxidation and reduction peaks confirming the proper immobilization of POxNPs onto Au electrode.

3.1.4. Characterization of POxNPs/AuE by EIS

EIS was implemented to scrutinize the immobilization of POxNPs onto AuE. The nyquist plot (Fig. 4b) explores the EIS of POxNPs/AuE in 5 mM potassium ferro/ferricyanide solution. The charge transfer resistance (R_{CT}) value for bare AuE was 250 ohms, which was lower than 370 ohms for POxNPs/AuE. These observed results were in direct correlation with the fact that an increase in R_{CT} value of POxNPs/AuE was due to covalent binding of POxNPs onto Au surface, and since biological molecules are known to be poor conductors of electricity thereby, they restraint the electron transfer.

3.2. Optimization of pyruvate biosensor

A novel amperometric pyruvate biosensor was fabricated based on the covalent immobilization of POxNPs onto AuE. The maximum current was recorded within 7.5 s at 0.28 V against Ag/AgCl. Therefore, in the proceeding electrochemical analysis, the current was recorded within 7.5 s at this voltage. The highest current response of fabricated biosensor was recorded at pH 5.5 (Fig. 5a), which is nearly similar to the optimum pH of the native enzyme (POx). At below and above pH 5.5, the response of the pyruvate biosensor decreased gradually. This might be possible due to decreased POx activity under these conditions. The optimum pH of present biosensor was lower than that of the earlier reported amperometric pyruvate biosensor based on POx immobilized onto Pt disc electrode [18], 3- MPA/ 6- ACA/ POx glutaraldehyde modified electrode [2]; POx immobilized in gelatin on YSI type dissolved oxygen probe [9]; redox hydrogel based biosensor [19], POx electrodeposited polytramine [20] and, almost similar to a biosensor based on POx immobilized on meldolas blue electrode [6]. On the other hand, the optimum temperature of biosensor recorded was 35°C (Fig. 5b.). The optimum temperature was analyzed within a range of 15–50° C and it was observed that with increasing temperature, the biosensor response was increased, which might be due to the increased kinetics of the reaction. This reached an optimum value at 35° C and thereafter, declined due to denaturation of enzyme. This was almost similar to the biosensor based on POx immobilized in gelatin (pO_2 electrode) as cited by Bacri and Burstein [21].

3.3. Evaluation of pyruvate biosensor

There was a linear relationship between pyruvate concentration in the range 0.01 µM to 5000 µM, under standard working conditions (Fig. 5c), after which it showed saturation. This observation is found to be one step ahead than the previously elucidated biosensors, which showed their working range between 10 µM– 5000 µM [18] 4 µM-120 µM [5], 2 µM-12 µM [6], 90 µM-600 µM [22], 5 µM – 5000 µM [20], 0 µM-2000 µM [23], 2 µM- 6 µM [19] respectively. The detection limit (LOD) of the present biosensor was 0.01 µM, which is far better than the previously outlined biosensors cited in the literature till date [2,5,9,18,21–24]. The analytical recoveries of added pyruvate in sera at levels of 1.0 mM and 2.0 mM were 99.0% and 99.5% respectively, signifying the reliable fabrication of the present biosensor (Table 2a). The pyruvate content was determined in serum samples repeatedly six times on the same day (within batch) and in the same samples after their storage at -20°C for one week (between batch) by present ENPs based electrode. The within and between batch coefficients of variation (CV) in serum pyruvate were 0.045% and 0.040% respectively (Table 2b). These highly precise values show that the present biosensor is an efficient and consistent model exhibiting good reproducibility, which could be attributed to the covalent immobilization of POxNPs onto Au electrode via thiolate bond. The thiolate bond between AuE and ENPs stabilizes the activity of enzyme, hence the reproducibility of enzyme electrode is enhanced [15].

3.4. Correlation of pyruvate biosensor

The levels of pyruvate in sera of apparently healthy individuals and persons under cardiogenic stress was detected by present biosensor and compared with those obtained by standard spectrophotometric method [11]. An excellent correlation coefficient ($R^2 = 0.99$) was obtained between the values by these two methods, with regression equation being $y = 0.9967x$ (Fig. 6). These observations expressed utmost accuracy of the present biosensor.

3.5. Applications of pyruvate biosensor

The level of pyruvate in sera of apparently healthy adults as detected by the present biosensor was between 42.0 µM ± 2.60 to 89.02 µM ± 2.09, which lies in the normal established range. The pyruvate level in sera of persons suffering from cardiogenic stress was detected in the range, 147.2 µM ± 2.71 to 212.4 µM ± 3.28, which is significantly

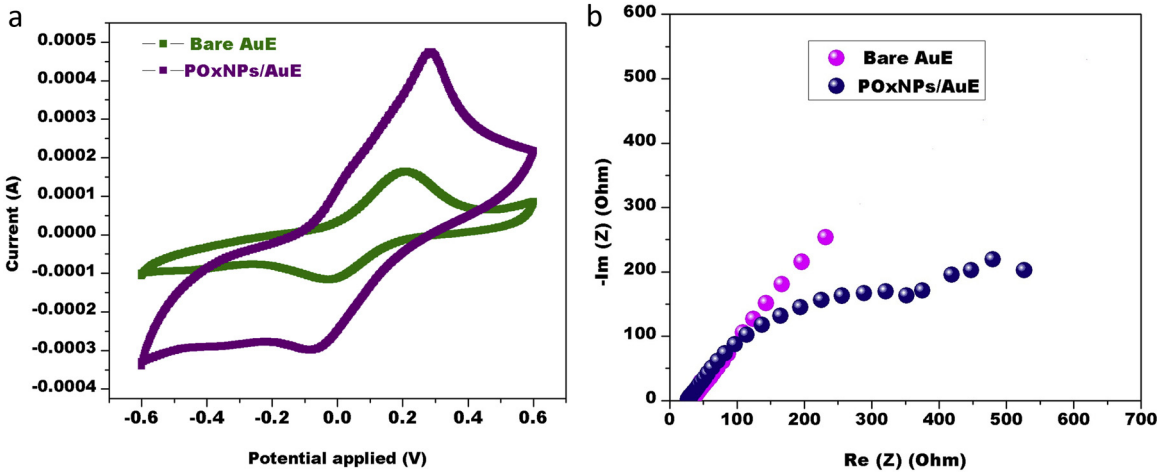

Fig. 4. (a) Cyclic voltammogram (CV) of POxNPs/Au electrode in 25 ml 0.1 M sodium phosphate buffer pH- 7.0 containing 0.1 ml of 0.1 M pyruvate solution, 10 µl TPP and 10 µl FAD and 10 µl $MgCl_2$ under standard conditions at a scan rate of 30 mVs^{-1} (b) Electrochemical impedance spectra (EIS) of (a) Bare AuE, (b) POxNPs modified gold electrode.

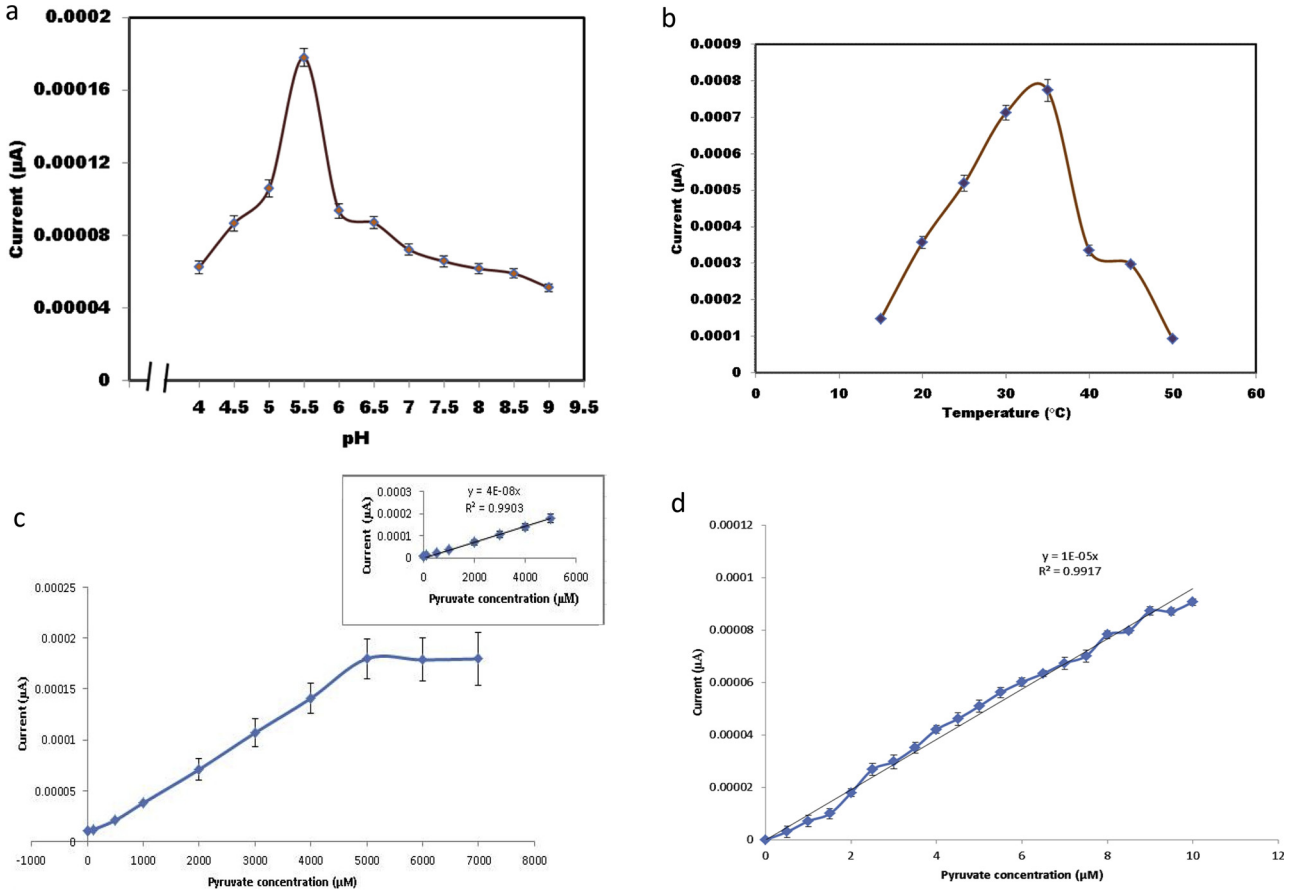

Fig. 5. (a) Influence of pH. (b). Influence of incubation temperature on the current response of POxNPs/ Au electrode in 25 ml 0.1 M sodium phosphate buffer (pH-7.0) containing 0.1 ml 0.1 M pyruvate solution 10 µl TPP and 10 µl FAD and 10 µl $MgCl_2$.(c) Effect of pyruvate on biosensor current response based on POxNPs/ AuE. **Inset of** Fig. 5**c.** Standard curve of pyruvate concentration by present biosensor based on POxNPs/ Au electrode, prepared in 25 ml 0.1 M sodium phosphate buffer (pH- 7.0) containing 0.1 ml of 0.1 M pyruvate solution, 10 µl of 10 mM TPP, 10 µl of 1 mM $MgCl_2$ and 10 µl of 1 µM FAD, under standard conditions. (d) Effect of pyruvate on biosensor current response based on POxNPs/AuE in lower concentration range.

elevated than those in apparently healthy adults (Table 3).

3.6. Interference study of pyruvate biosensor

The interfering activity of several components was analyzed to determine the selectivity and specificity of the present biosensor. The POxNPs/AuE biosensor unveiled excellent anti- interference ability with several chief blood components such as urea, uric acid, ascorbic acid, glucose and lactic acid at their physiological concentrations. Addition of uric acid and lactic acid practically had no effect on biosensor response, which can be attributed to the usage of low potential (0.28 V) during experimentation. On the contrary, other components

Table 2a
Analytical recovery of added pyruvate in the serum samples (n = 5), as measured by pyruvate biosensor based on POxNPs/ Au electrode (POx- Pyruvate oxidase, NPs- Nanoparticles).

Pyruvate added	Pyruvate found ((μM)	% Recovery
–	59	100
1 mM	59.4	99 ± 0.01
2 mM	60.7	99.5 ± 0.03

Table 2b
Within and between batch assay coefficients of variation for determination of pyruvate in the serum samples, as measured by pyruvate biosensor based on POxNPs/Au electrode (POx- Pyruvate oxidase, NPs- Nanoparticles).

N; Pyruvate (μM)	Pyruvate (μM); mean	CV (%)
Within assay (n = 5)		
70	**66.0**	**0.045**
63		
62		
68		
67		
Between batch (n = 5)		
78	**74.4**	**0.040**
69		
75		
76		
74		

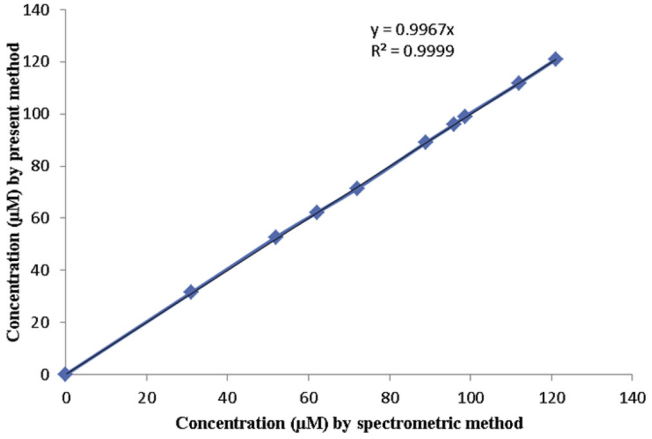

Fig. 6. Correlation curve between sera pyruvate values as measured by standard spectrophotometric (X- axis) method and the present biosensor (Y- axis) based on POxNPs/AuE.

like urea, ascorbic acid and glucose showed only by 5.18%, 5.06% and 8.004% interference respectively. The biosensor showed negligible interference (0–10%) in its activity in presence of all possible interfering substances. However, it showed current response only in the presence of pyruvate revealing the specificity and selectivity for pyruvate detection.

3.7. Reusability of POxNPs/Au electrode

The initial activity of POxNPs/AuE (working electrode) diminished just by 25% after its continual use over a period of 240 days, while being stored at 4°C . These observations point towards the better stability of the present ENPs based electrode than that cited by others in literature, 42 days [18]; 90 days with no loss in activity [20]; > 60 days [3] and > 10 days (100 assays) [25].

4. Conclusions

In the present work, the application of enzyme nanoparticles (ENPs) in place of native enzymes/free enzyme molecules has resulted into better analytic performance of amperometric pyruvate biosensor in terms of working range (0.01–5000 μM), limit of detection (0.67 μM), short response time (7.5 s), negligible and severely low interference activity by other blood components and enhanced storage stability (240 days). Based on these outcomes, it can be inferred that the use of ENPs of POx has helped to overcome the barriers caused by the previously available electrochemical biosensors. Further, direct immobilization of ENPs onto Au electrode simplified the process of fabrication of nanomaterial- based biosensors. The current work lacks the miniaturization of biosensor. The future research could be focused on the development of microfluidic paper based pyruvate biosensor, which could be used at the bedside of the patients for point of care (POC) analysis of serum pyruvate.

Conflict of interest

The authors have no conflict of interest.

Author's agreement

This is to certify that all authors **Mansi Malik[a], Reeti Chaudhary[a] and C.S. Pundir[b*]** have seen and approved the final version of the manuscript entitled **"An improved enzyme nanoparticles based amperometric pyruvate biosensor for detection of pyruvate in serum".** The authors warrant that the work has not been published before and has not been submitted to any other journal for consideration of its publication. Also, the authors declare no conflict of interest.

Acknowledgement

The authors are highly grateful to the Directors of Pt. BDS Post Graduate Institute of Medical Science (PGIMS), Rohtak, Noble Heart hospital and Holy Heart hospital, Rohtak for providing sera samples of apparently healthy persons and cardiogenic patients used in the present research work. We also thank Dr. Rajvinder Singh, Assistant Professor, Department of Genetics, M.D.U., Rohtak, for FTIR spectroscopy.

Table 3
Serum pyruvate levels of apparently healthy adults and persons suffering from cardiogenic stress, as measured by pyruvate biosensor based on POxNPs/ Au electrode (POx- Pyruvate oxidase, NPs- Nanoparticles).

Age group	Healthy (μM)				Diseased (μM)			
	Male	n	Female	n	Male	n	Female	n
30-40	65.0 ± 2.32	5	47.4 ± 1.85	5	347.2 ± 2.71	5	154.6 ± 5.17	5
40-50	76.0 ± 1.33	5	83.0 ± 2.28	5	253.4 ± 3.32	5	160.6 ± 2.07	5
50-60	93.8 ± 1.65	5	69.0 ± 1.41	5	159.0 ± 1.23	5	167.4 ± 2.40	5
60-70	58.0 ± 1.41	5	77.4 ± 2.21	5	184.4 ± 3.43	5	173.0 ± 3.80	5
70-80	98.6 ± 1.62	5	88.8 ± 2.78	5	401.6 ± 1.06	5	206.0 ± 7.03	5
80-90	108.0 ± 1.86	5	119.0 ± 2.10	5	283.2 ± 3.01	5	212.4 ± 3.2	5

References

[1] F. Shapiro, N. Silanikove, Rapid and accurate determination of malate, citrate, pyruvate and oxaloacetate by enzymatic reactions coupled to formation of a fluorochromophore: application in colorful juices and fermentable food (yogurt, wine) analysis, Food Chem. 129 (2011) 608–613.

[2] E. Bayram, E. Akyilmaz, A new pyruvate oxidase biosensor based on 3-mercaptopropionic acid/6-aminocaproic acid modified gold electrode, Artif. Cells, Nanomed. Biotechnol. 42 (2013) 418–422.

[3] J. Kulys, L. Wang, N. Daugvilaite, Amperometric methylene green-mediated pyruvate electrode based on pyruvate oxidase entrapped in carbon paste, Anal. Chim. Acta 265 (1992) 15–20.

[4] L.R. Gray, S.C. Tompkins, E.B. Taylor, Regulation of pyruvate metabolism and human disease, Cell. Mol. Life Sci. 71 (2014) 2577–2604.

[5] Y.-S. Li, Q.-J. Li, W. Yang, X.-F. Gao, Research on a new micro-volume fluorescence capillary biosensor assay for sequentially quantifying pyruvate and lactate, J. Fluoresc. 27 (2017) 883–894.

[6] L. Abayomi, L. Terry, S. White, P. Warner, Development of a disposable pyruvate biosensor to determine pungency in onions (Allium cepa L.), Biosens. Bioelectron. 21 (2006) 2176–2179.

[7] W. Li, C. Pan, T. Hou, X. Wang, F. Li, Selective and colorimetric detection of pyruvic acid using conformational switch of i-motif DNA and unmodified gold nanoparticles, Anal. Methods 6 (2014) 1645.

[8] M.M. Essa, S. Subash, N. Braidy, S. Al-Adawi, C.K. Lim, T. Manivasagam, G.J. Guillemin, Role of NAD+, oxidative stress, and tryptophan metabolism in autism spectrum disorders, Int. J. Tryptophan Res. 6 (2013) 15–28.

[9] E. Akyilmaz, E. Yorganci, A novel biosensor based on activation effect of thiamine on the activity of pyruvate oxidase, Biosens. Bioelectron. 23 (2008) 1874–1877.

[10] G.E. Anthon, D.M. Barrett, Modified method for the determination of pyruvic acid with dinitrophenylhydrazine in the assessment of onion pungency, J. Sci. Food Agric. 83 (2003) 1210–1213.

[11] S. Berntsson, Spectrophotometric Determination of Pyruvic Acid by the Salicylaldehyde Method, Anal. Chem. 27 (1955) 1659–1660.

[12] C. Olsen, An en ymatic fluorimetric micromethod for the determination of acetoacetate β- Hydroxybutyrate, pyruvate and lactate, Clin. Chim. Acta 33 (1971) 293–300.

[13] K.S. Yoo, L.M. Pike, Development of an automated system for pyruvic acid analysis in onion breeding, Sci. Hortic. (Amsterdam). 82 (1999) 193–201.

[14] A.P.F. Turner, Biosensors: sense and sensibility, Chem. Soc. Rev. 42 (2013) 3184–3196.

[15] C.S. Pundir, Enzyme Nanoparticles: Preparation, Characterization, Properties and Application, Elsevier, London, 2015, pp. 5–60.

[16] K. Dagar, C.S. Pundir, Covalent Immobilization of Lactate Oxidase onto Zirconia Coated Silica Nanoparticles/Chitosan Hybrid Film for Amperometric Determination of Lactate, Biochem. Anal. Biochem. 05 (2016) 1–9.

[17] G. Liu, Y. Lin, V. Ostatná, J. Wang, Enzyme nanoparticles-based electronic biosensor, Chem. Commun. (Camb.) 27 (2005) 3481–3483.

[18] D.V. Knyzhnykova, Y.V. Topolnikova, I.S. Kucherenko, O.O. Soldatkin, Development of pyruvate oxidase-based amperometric biosensor for pyruvate determination, Biopolym. Cell 34 (2018) 14–23.

[19] N. Gajovic, G. Binyamin, A. Warsinke, F.W. Scheller, A. Heller, Operation of a miniature redox hydrogel-based pyruvate sensor in undiluted deoxygenated calf serum, Anal. Chem. 72 (2000) 2963–2968.

[20] M. Situmorang, J.J. Gooding, D.B. Hibbert, D. Barnett, The development of a pyruvate biosensor using electrodeposited polytyramine, Electroanalysis. 14 (2002) 17–21.

[21] A.M. Zapata-Bacri, C. Burstein, Enzyme electrode composed of the pyruvate oxidase from Pediococcus species copuled to an oxygen electrode for measurement of pyruvate in biological media, Biosensors 3 (1987) 227–237.

[22] M.E. Ghica, C.M.A. Brett, Development of novel glucose and pyruvate biosensors at poly(neutral red) modified carbon film electrodes. Application to natural samples, Electroanalysis 18 (2006) 748–756.

[23] A.F. Revzin, K. Sirkar, A. Simonian, M.V. Pishko, Glucose, lactate, and pyruvate biosensor arrays based on redox polymer/oxidoreductase nanocomposite thin-films deposited on photolithographically patterned gold microelectrodes, Sens. Actuators B Chem. 81 (2002) 359–368.

[24] A. Maines, M.I. Prodromidis, S.M. Tzouwara-karayanni, M.I. Karayannis, D. Ashworth, An enzyme electrode for extended linearity citrate measurements based on modified polymeric membranes, Electroanalysis (2000) 1118–1123.

[25] F. Mizutani, K. Tsuda, I. Karube, S. Suzuki, K. Matsumoto, Determination of glutamate pyruvate transaminase and pyruvate with an amperometric pyruvate oxidase sensor, Anal. Chim. Acta 118 (1980) 65–71.

[26] F. Mizutani, S. Yabuki, Y. Sato, T. Sawaguchi, S. Iijima, Amperometric determination of pyruvate, phosphate and urea using enzyme electrodes based on pyruvate oxidase-containing poly(vinyl alcohol)/polyion complex-bilayer membrane, Electrochim. Acta 45 (2000) 2945–2952.